Available online at www.sciencedirect.com
ScienceDirect
Journal of Environmental Sciences 2013, 25(10) 2093–2101
JOURNAL OF ENVIRONMENTAL SCIENCES
ISSN 1001-0742
CN 11-2629/X
www.jesc.ac.cn

Electrochemical and spectroscopic characteristics of dissolved organic matter in a forest soil profile

Ran Bi[1,2], Qin Lu[2], Tian Yuan[2], Shungui Zhou[2,*], Yong Yuan[2], Yanfei Cai[3]

1. Guangzhou Institute of Geochemistry, Chinese Academy of Sciences, Guangzhou 510640, China. E-mail: br19870805@sina.com
2. Guangdong Institute of Eco-Environmental and Soil Sciences, Guangzhou 510650, China
3. College of Resources and Environment, South China Agricultural University, Guangzhou 510642, China

Received 09 January 2013; revised 06 March 2013; accepted 13 March 2013

Abstract

Dissolved organic matter (DOM) represents one of the most mobile and reactive organic compounds in ecosystem and plays an important role in the fate and transport of soil organic pollutants, nutrient cycling and more importantly global climate change. Electrochemical methods were first employed to evaluate DOM redox properties, and spectroscopic approaches were utilized to obtain information concerning its composition and structure. DOM was extracted from a forest soil profile with five horizons. Differential pulse voltammetry indicated that there were more redox-active moieties in the DOM from upper horizons than in that from lower horizons. Cyclic voltammetry further showed that these moieties were reversible in electron transfer. Chronoamperometry was employed to quantify the electron transfer capacity of DOM, including electron acceptor capacity and electron donor capacity, both of which decreased sharply with increasing depth. FT-IR, UV-Vis and fluorescence spectra results suggested that DOM from the upper horizons was enriched with aromatic and humic structures while that from the lower horizons was rich in aliphatic carbon, which supported the findings obtained by electrochemical approaches. Electrochemical approaches combined with spectroscopic methods were applied to evaluate the characteristics of DOM extracted along a forest soil profile. The electrochemical properties of DOM, which can be rapidly and simply obtained, provide insight into the migration and transformation of DOM along a soil profile and will aid in better understanding of the biogeochemical role of DOM in natural environments.

Key words: dissolved organic matter; electrochemical characteristics; soil profile; spectroscopic characteristics
DOI: 10.1016/S1001-0742(12)60283-6

Introduction

Dissolved organic matter (DOM) represents one of the most mobile and reactive organic matter fractions in ecosystem. DOM as a heterogeneous mixture of organic molecules with different sizes, structures and functional properties is often defined operationally as "the part of organic matter that is able to pass through a filter with a pore size of 0.45 μm" (Zsolnay, 2003). DOM consists of low molecular weight substances, such as organic acids and amino acids, as well as complex molecules of high molecular weight, such as humic substances and enzymes.

DOM is widely distributed in the natural environment, where it plays a significant role in the fate and transport of pollutants (e.g. heavy metals and persistent organic pollutants) and in nutrient cycling (Chen et al., 1996; Zhou et al., 2004). Earlier researchers primarily focused on the complexation and adsorption properties of DOM (Zhan et al., 2010). Recently, its redox properties have drawn a great deal of interest because of its capability of mediating biogeochemical redox reactions associated with the fate of environmental pollutants (Blodau et al., 2009; Zhang and Weber, 2009) and cycling of soil carbon (Heitmann et al., 2007). DOM can function as electron shuttle for continuous electron transfer between electron donor and electron acceptor. Electrochemical approaches have been proven to be useful tools for rapidly and accurately evaluating the redox properties of DOM, by which many important parameters are obtainable, including electron transfer capability (ETC), electron transfer reversibility, redox potentials and so forth (Nurmi and Tratnyek, 2002; Yuan et al., 2011).

In a forest ecosystem, organic matter in forms of plant litter, soil humus, microbial biomass and root exudates accumulates in the top soil layer (Kalbitz and Kaiser, 2008) and undergoes mineralization and humification with DOM migrating down the soil profile (Corvasce et al.,

* Corresponding author. E-mail: sgzhou@soil.gd.cn

2006; Kaiser and Kalbitz, 2012). Studies have been carried out to investigate the distribution, biodegradation, physiochemical and biogeochemical properties of DOM along soil profiles (Kalbitz et al., 2005; Corvasce et al., 2006). However, few studies have tried to characterize the electrochemical properties of DOM along a soil profile, which are important for understanding soil biogeochemistry in a vertical direction. Therefore, this research was carried out in an attempt to fill the gap.

Herein, we aimed to: (1) investigate changes in the redox properties of DOM along the profile using electrochemical approaches; (2) characterize the composition and structure of DOM by means of spectroscopic techniques; and (3) analyse the relationship between the electrochemical and spectroscopic characteristics of DOM.

1 Materials and methods

1.1 Site description and sample properties

The selected site is located in the Nankun Mountain (23°39′N, 113°54′E), Huizhou, Guangdong Province, China, with an altitude of 455 m above sea level. The climate is mild all the year with a mean annual rainfall of 2700 mm and an average temperature of 23°C. The forest community of the area belongs to south subtropical montane evergreen broadleaf forest. Dominant tree species are *Cunninghamia lanceolata* and *Phyllostachys heterocycla* with undergrowth consisting mainly of *Dicranopteris pedata* and *Rhodomyrtus tomentosa*.

The soil develops from granite. The soil profile of typic ali-udic argosols was characterized by three distinct soil horizons designated as: a humus eluvial horizon (A), an enriched illuvial horizon (B) and a weathered horizon (C) and an intermediate AB layer between the A and the B horizons. The B horizon was also further divided into an upper strongly illuvial B1 and a lower partially illuvial B2. The soil horizons were distinguished by their color and found at the following average depths: 0–18 cm for A, 18–30 cm for AB, 30–68 cm for B1, 68–115 cm for B2 and 115–130 cm for C (**Fig. 1**).

In the laboratory, after visible roots and plant fragments were removed, soil sample from each horizon was air-dried, passed through a 2-mm sieve, and then stored at room temperature in airtight polyethylene containers until analyzed. Particle size distribution was analyzed by the hydrometer method (Chen et al., 2010). Soil pH was measured in a 2.5:1 water/dry soil suspension using a pH meter (Bi et al., 2010). Total organic carbon (TOC) and total nitrogen (TN) content were determined with the potassium dichromate method and semimicro Kieldahl method (Bi et al., 2010; Chen et al., 2010), respectively.

1.2 DOM extraction

DOM was extracted as previously reported by Yuan et al. (2011). Briefly, DOM was extracted with distilled water

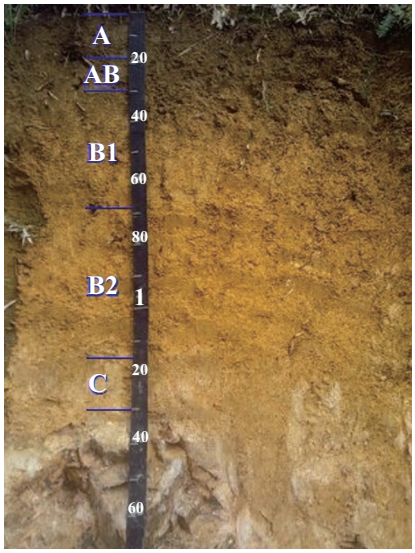

Fig. 1 Photo of the forest soil profile with five horizons (A, 0–18 cm; AB, 18–30 cm; B1, 30–68 cm; B2, 68–115 cm and C; 115–130 cm).

at a solid/water ratio of 1:5 (W/V, dry weight basis) in a reciprocal shaker (200 r/min) for 16 hr at 20°C. The suspension was subsequently centrifuged at 12,000 r/min for 20 min and thereafter the supernatant was filtered through a 0.45 μm sterile membrane (GN-6 Metrice, Gelman Sciences, Ann Arbor, MI, USA). Dissolved organic carbon (DOC) was measured with a TOC digital reactor block (DRB200, HACH, USA) equipped with a spectrophotometer (DR2700, HACH, USA). Part of the extracted DOM was freeze-dried for fourier transform infrared (FT-IR) spectroscopy (Vector33, Brnker Optics, Germany) and cyclic voltammetry analyses. The left was stored at 4°C before used for differential pulse voltammetry (DPV) and chronoamperometry measurements. For ultraviolet-visible (UV-Vis) (TU-1810, Persee, China) and fluorescence spectroscopy (F-4600, Hitachi, Japan), DOM solution was diluted to 15.0 mg C/L.

1.3 Electrochemical measurements

Electrochemical experiments were performed using an electrochemistry workstation CHI660D (Chenhua Co. Ltd., Shanghai, China) with a conventional three-electrode cell at ambient temperature. DPV was applied for detecting redox active groups as reported by Zhang et al. (2009). Glass carbon, Pt wire and Hg/Hg_2Cl_2 were used as working, counter and reference electrodes, respectively. Nine mL DOM solution was transferred to the electrochemical cell, and 1.00 mL of 5.00 mmol/L ammonium acetate was added as supporting electrolyte. The operating conditions to obtain voltammograms included a scan speed of 10 mV/sec, a pulse voltage of 50 mV, and an operating voltage range of –0.5~+1.0 V. During sampling and determination, the head space of the electrochemical cell was flushed with pure nitrogen to prevent reduced DOM from oxidation. Cyclic voltammecry for measuring electron transfer reversibility was performed with Pt disk (3 mm in diameter)

as working electrode, Pt wire as counter electrode, and Hg/Hg_2Cl_2 electrode as reference electrode. A scan rate of 5 mV/sec in the potential range of –1.5 to +0.5 V was applied. Dimethyl sulfoxide was used as the solvent and 1.00 mmol/L $NaClO_4$ as the electrolyte (Nurmi and Tratnyek, 2002). Chronoamperometry measurements were performed to quantify the electron transfer capability (ETC) of DOM in a N_2-saturated phosphate buffer solution (pH 7.00) at applied potentials under stirring as suggested by Yuan et al. (2011). A graphite plate with a projected surface area of 17.50 cm^2 was used as the working electrode, and Pt wire and Hg/Hg_2Cl_2 as the counter and reference electrodes, respectively. A positive potential of 0.5 V (vs. Hg/Hg_2Cl_2) was applied for electron donor capacity (EDC) measurement and a potential of –0.6 V (vs. Hg/Hg_2Cl_2) for electron acceptor capacity (EAC).

1.4 Spectroscopic analyses

FT-IR, UV-Vis, and fluorescence spectroscopy were used to obtain structural information of the extracted DOM. Infrared absorption spectra from 4000–400 cm^{-1} were recorded on a Hitachi EPI infrared spectrophotometer using the KBr disk method. UV-Vis absorbance was measured with a spectrophotometer from 200 to 600 nm with quartz cuvettes. Three-dimensional excitation/emission matrix (3DEEM) fluorescence spectra were recorded with a fluorescence spectrophotometer equipped with a 150 W xenon arc lamp as the excitation source. A photomultiplier tube voltage of 700 V and an automatic response time were applied. The slit widths were 10 nm for both excitation and emission monochromators, and the scan speed was kept at 1200 nm/min. Wavelengths were set from 200 to 500 nm for excitation and 250 to 600 nm for emission. Samples were kept at constant temperature ((20 ± 1)°C in water bath) before being placed into the quartz cells. Sigma Plot software was used to obtain the 3DEEM spectra. To obtain the humification index (HIX) of the samples, fluorescence spectroscopy was also run at the excitation wavelength of 254 nm and emission wavelength from 200 to 500 nm.

2 Results

2.1 Distribution of DOM along the soil profile

Selected chemical and physical properties of the forest soil profile studied are reported in **Table 1**. A slight increase of pH was observed along the lower portion of the profile, even though pH of horizon A was slightly higher than that of horizon AB. As expected, TOC and TN decreased with increasing depth. C/N ratio also dropped along the profile.

Table 1 also shows the distribution of DOC along the profile. Similar to TOC, DOC also decreased with increasing soil depth: rapidly from 143.00 mg/L in horizon A to 41.00 mg/L in horizon AB and then slowly from 20 mg/L in horizon B1 to 15.00 mg/L in horizon C. Although both TOC and DOC decreased with increasing soil depth, DOC/TOC did not have the same trend. Instead, DOC/TOC first decreased from 2.84% in horizon A to 1.18% in horizon AB and then increased. DOC/TOC in horizon C (3.91%) was even higher than that in horizon A.

2.2 Electrochemical characteristics of DOM

2.2.1 Changes of redox active moieties

DPV as the most sensitive voltammetry can distinguish different redox active moieties through peak numbers and potentials. **Figure 2a** shows that DOM from upper layers contained more redox-active functional groups. There were 3 groups of redox-active moieties with different potentials presenting in the DOM extracted from horizon A, AB and B1, while in horizon B2, only 2 of the 3 were still detected. And further down to the C horizon, only 1 group remained.

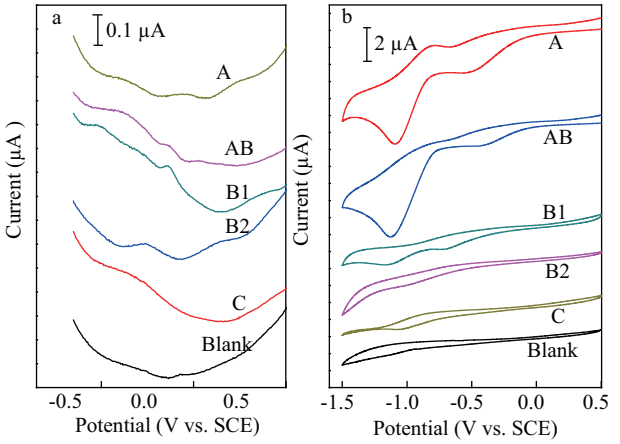

Fig. 2 Voltammograms of the DOM extracted from each horizon of the soil profile with counter electrode: Pt wire and reference electrode: Hg/Hg_2Cl_2. (a) differential pulse voltammograms (glass carbon as working electrode, 5.0 mmol/L ammonium acetate as electrolyte and scan rate of 10 mV/sec); (b) cyclic voltammograms (Pt disk (3 mm in diameter) as working electrode, 1.0 mmol/L $NaClO_4$ as electrolyte and scan rate of 5 mV/sec).

Table 1 Main chemical and physical properties of the soil profile

Horizon	Depth (cm)	pH (H_2O)	TOC (g/kg)	TN (g/kg)	DOC		C/N ratio	DOC/TOC (%)	Sand (%)	Silt (%)	Clay (%)
					(g/kg)	(mg/L)					
A	0–18	4.42	25.20	1.89	0.715	143.00	13.33	2.84	52.75	18.65	28.60
AB	18–30	4.32	17.31	1.44	0.205	41.00	12.02	1.18	47.52	16.32	36.16
B1	30–68	4.33	7.46	0.61	0.100	20.00	12.23	1.34	49.53	17.66	32.81
B2	68–115	4.50	5.84	0.60	0.095	19.00	9.73	1.63	49.64	15.28	34.05
C	115–130	4.86	1.92	0.42	0.075	15.00	4.57	3.91	75.43	9.18	15.39

2.2.2 Electron transfer reversibility

A typical cyclic voltammogram exhibits a pair of peaks, indicating reversibility of electron transfer. Completely symmetrical pairs donate fully reversibility, while incompletely symmetrical pairs suggest partly reversible. As shown in **Fig. 2b**, there were two pairs of well-defined peaks for DOM from horizon A, AB and B1 and the peaks were close-by. In contrast, only one pair of weakly defined peaks showed up for DOM from horizon B2 and C. These pairs were not completely symmetrical. **Figure 2b** also shows that the DOM from an upper layer caused a bigger change in current, which indicated higher concentrations of redox active moieties at the electrode surface (Nurmi and Tratnyek, 2011).

2.2.3 Electron transfer capacity

ETC of DOM, including EAC and EDC, has been widely studied (Bauer et al., 2007; Yuan et al., 2011). EAC or EDC was defined as the number of mole equivalents of electrons transferred to or withdrawn from DOM normalized to soil dry weight at a given potential. As shown in **Fig. 3a**, DOM from an upper layer had a higher EAC or EDC, except that DOM from horizon C had an slightly higher EAC than that from horizon B2. DOM from horizon A had EAC of 530.34 μmol e^-/kg soil which was nearly 5 times that from horizon AB and 7 times that from the lower 3 layers. EDC of DOM from different layers was in a range from 91.78 to 11.71 μmol e^-/kg soil (**Fig. 3b**).

2.3 Spectroscopic characteristics of DOM

2.3.1 FT-IR spectroscopy and functional groups

The FT-IR spectra of the DOM extracted from different horizons was exhibited by number of peaks and peak intensity (**Fig. 4**). The functional groups were identified according to published results (Kanokkantapong et al., 2006; Huo et al., 2008). All spectra featured a broad band at 3390 cm^{-1}, which can be attributed to O–H stretching

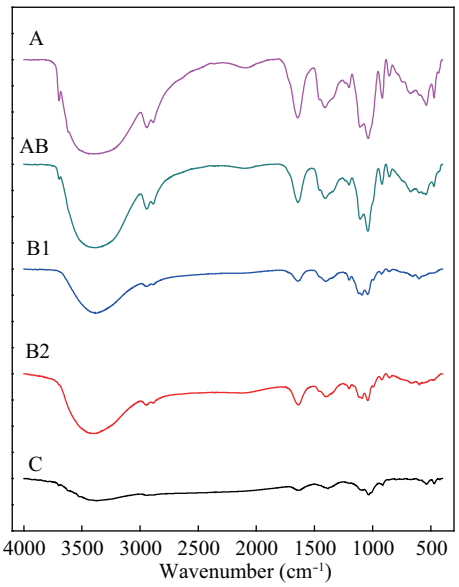

Fig. 4 FT-IR spectra of the DOM extracted from each horizon (A, AB, B1, B2, C).

from the presence of alcohols and/or phenols, and N–H stretching from amines and/or amides. In addition, the C–O and C–H stretching peaking at 1400 and 1250–1150 cm^{-1} decreased sharply with increasing soil depth, indicating decreasing concentrations of alcohols, phenols and/or carbohydrates. High intensity of the aromatic C=C and C=O of amide groups at 1690–1600 cm^{-1} of the upper horizons suggested the enrichment of aromatic and humic structures in the upper layers. It could be seen that the spectrum of DOM from an upper layer contained more peaks with higher intensity.

2.3.2 UV-Vis spectroscopy and aromaticity index

The UV-Vis spectrum of the DOM extracted from each horizon is presented in **Fig. 5**. As reported by others, the spectra were featureless with absorbance decreasing

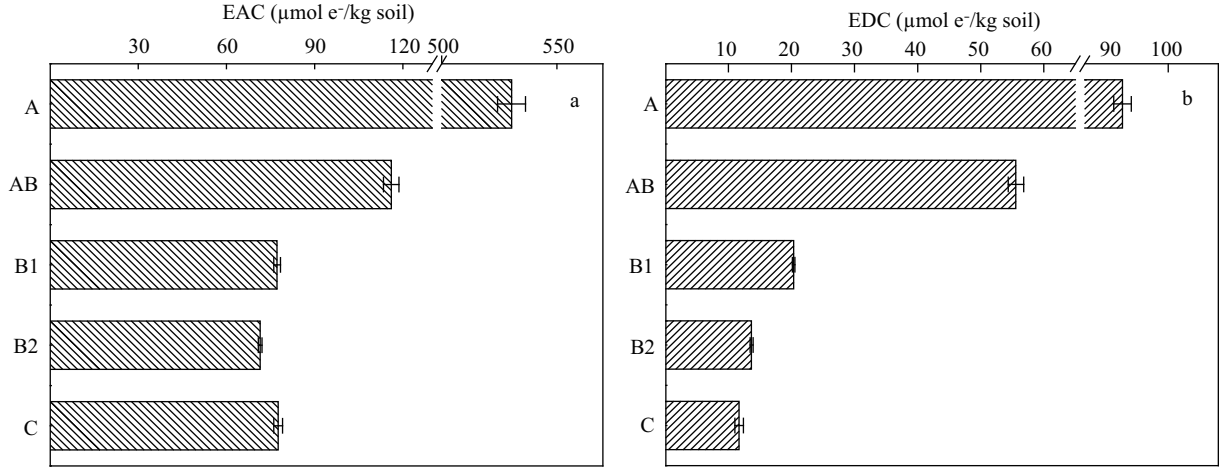

Fig. 3 Electron transfer capacities of the DOM extracted from each horizon. (a) electron acceptor capacity at a negative potential of –0.6 V (vs. Hg/Hg_2Cl_2); (b) electron donor capacity at a positive potential of 0.5 V (vs. Hg/Hg_2Cl_2). Mean and standard deviation of three replicates for each sample.

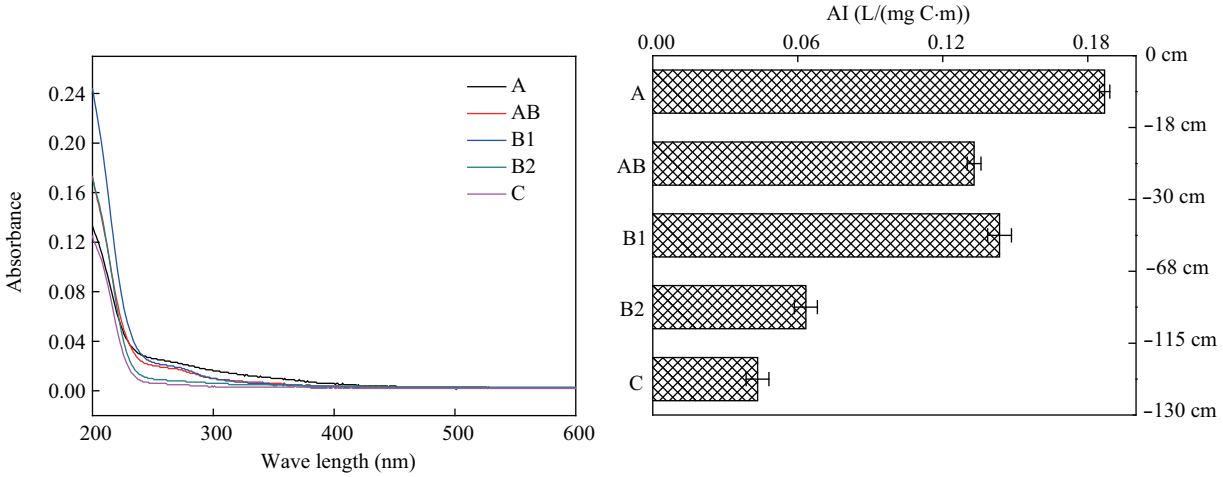

Fig. 5 UV-Vis spectra and aromaticity index (AI) of the DOM extracted from each horizon. Mean and standard deviation of three replicates for each sample.

rapidly with increasing wavelength. However, a number of quantitative metrics derived from UV-Vis spectra have proven to be useful in providing information concerning DOM's structure. The specific UV absorbance at 254 nm ($SUVA_{254}$) was reported to have a strong relationship with the degree of aromaticity and therefore aromaticity index (AI) was defined and calculated as (UV_{254}/DOC) × 100 (Corvasce et al., 2006). The AI of DOM from horizons A, AB, B1, B2 and C was 0.19, 0.13, 0.14, 0.06 and 0.04 L/(mg C·m), respectively (**Fig. 5**), suggesting that DOM from upper horizons contained a relatively high amount of aromatic structures while DOM from lower horizons was richer in aliphatic carbon.

2.3.3 Fluorescence spectroscopy and humification index

Three-dimensional excitation/emission matrix fluorescence spectra of DOM extracted from each horizon of the soil profile are shown in **Fig. 6**. Three different fluorophores, not necessarily occurring simultaneously in all horizons, could be observed in the EEM spectra. In general, peaks at shorter excitation wavelengths (< 250 nm) and shorter emission wavelengths (< 350 nm) were related to simple aromatic proteins such as tyrosine (Chen et al., 2003; Guo et al., 2010). Peaks in the range of Ex/Em 250–280 nm/320–360 nm were related to soluble microbial by product-like materials and simple phenolic compounds with the conjugated electronic system limited to one aromatic ring (Chen et al., 2003). Peaks in the range of Ex/Em 240–260 nm/380–480 nm as well as of Ex/Em 320–350 nm/400–480 nm were associated with humic- and fulvic-like substances (Cory and Mcknight, 2005; Cawley et al., 2012). As presented in **Fig. 6** the main peaks of DOM indicated humic- and fulvic-like substances and the fluorescence intensity of horizon A were much higher than that of horizon AB. However, the fluorescent regions of the lower three horizons B_1, B_2 and C were dominated by moieties of simple aromatic proteins analogue and simple phenolic.

The humification index is defined as the ratio of the area in the upper quarter (∑435–480 nm) to the area in the lower usable quarter (∑300–345 nm) of the usable fluorescence emission spectrum at the excitation of 254 nm (Zsolnay et al., 2003). The HIX of DOM from an upper layer was bigger than that from a lower layer except that HIX of DOM from horizon C was bigger than that from horizon B2 (**Fig. 7**). HIX of horizon A was over 3, decreasing to about 1 in the lower 2 horizons.

3 Discussion

Soil acts towards DOM as a chromatographic system, with the more sorptive compounds being retained and the more mobile ones being leached (Kalbitz and Kaiser, 2012). The decreased DOC concentration down the soil profile might be attributed to the sorption of DOM on reactive surfaces of plant-derived compounds in near surface compartments and the mineral matrix of the horizons (Kaiser and Guggenberger, 2000). Cervantes et al. (2000) had obtained similar results and draw the conclusion that strong physico-chemical interactions could occur between DOM and the mineral surfaces in the profile. High microbial activity, high fungal abundance, high carbon content and other favorable conditions in the top soil layer boosting mineralization all lead to a high DOM concentration. And, during migration down the profile, DOM was not only subjected to physico-chemical sorption or/and co-precipitation but also subjected to microbial processing and subsequent biodegradation (Kalbitz et al., 2005). DOC/TOC ratio was not only associated with soil minerals but also with organic carbon compositions and microbial activities. For horizon AB, which had the highest clay content, DOC/TOC was the lowest. As less complex and more water extractable organic compounds can move easily along the soil profile and lower microbial activities down the profile, DOC takes

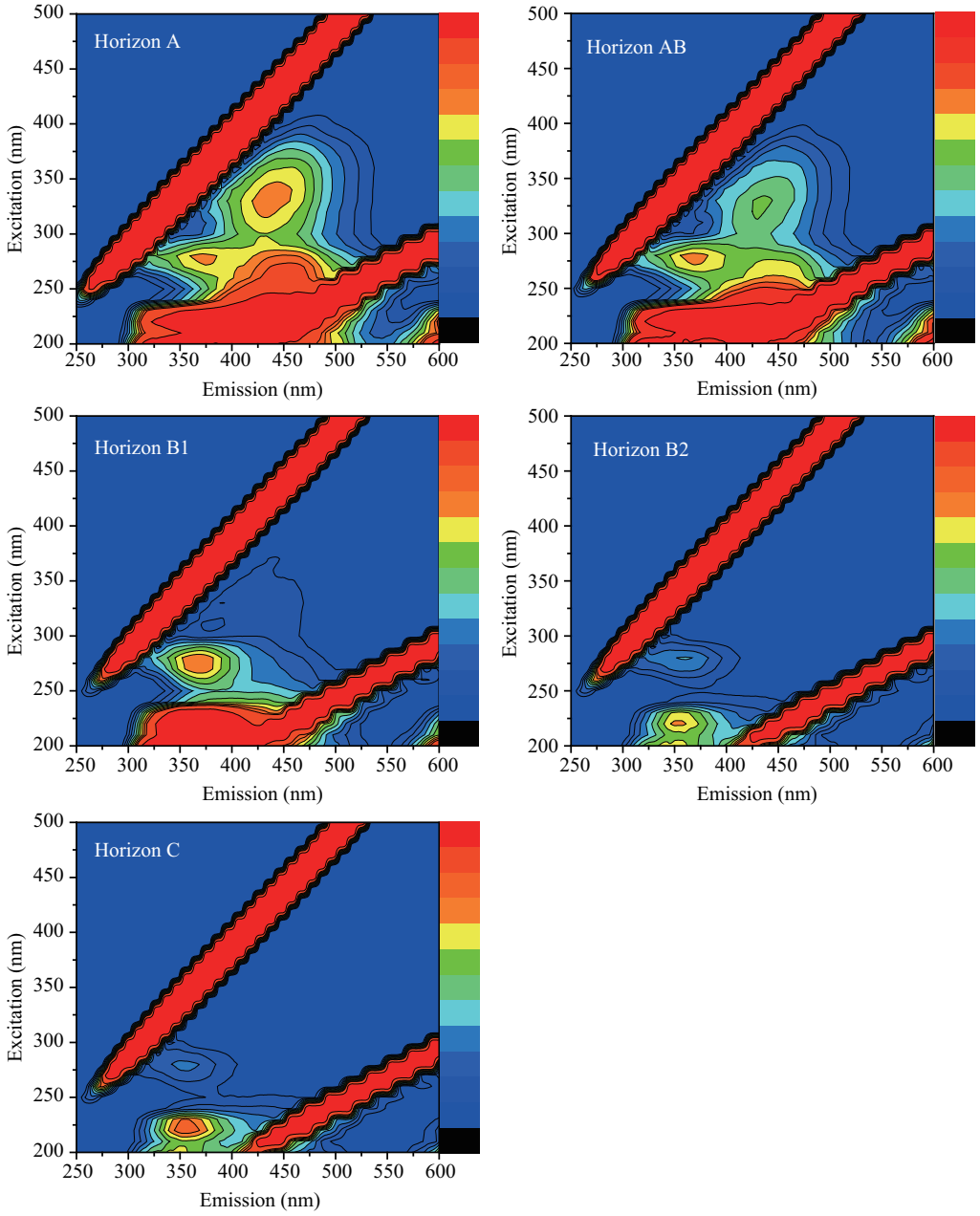

Fig. 6 3DEEM spectra of the DOM extracted from each horizon: A, AB, B1, B2, and C. 10 nm for both slit widths of excitation and emission, and the scan speed of 1200 nm/min.

up a larger proportion of TOC in a lower layer.

The composition of DOM extracted from different horizons was different, which was reflected by the spectra obtained. As seen from the FT-IR spectra (**Fig. 4**), all the peaks decreased in intensity with increasing soil depth and some functional moieties disappeared in the subsoil, especially the aromatic C=C and C=O of amide groups that contribute to the aromatic and humic degree of DOM. The 3DEEM fluorescence spectra of DOM from the first two horizons indicated humic- and fulvic-like fluorophores that were typical of complex DOM, whereas the spectra of DOM from the lower horizons suggested simple structure fluorophores such as aromatic proteins analogue and phenols (Rumpel et al., 2004). AI and HIX decreased down the profile which was similar to the discovery by Corvasce et al. (2006). They believed that more complex and/or aromatic components of DOM were relatively less mobile and thus were preferentially retained onto soil mineral surfaces while simple and hydrophilic moieties were more mobile and were able to migrate towards deeper soil horizons. The spectroscopic results suggested DOM from upper layers was rich in complex substances derived from lignin or humus, while that from subsoil was dominated by simple carbohydrates and nitrogen rich compounds.

DOM are redox-active natural organic compounds that contribute to biogeochemical redox reactions, including

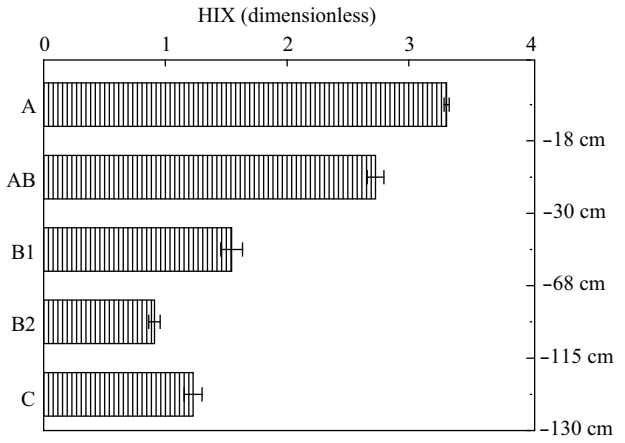

Fig. 7 Humification index (HIX) of the DOM extracted from each horizon. Mean and standard deviation of three replicates for each sample.

the transfer of electrons from microorganisms to poorly accessible mineral phases, such as Fe(III) oxides (Lovley et al., 1996; Bauer and Kappler, 2009), and from abiotic reductants to organic pollutants (e.g., halogenated hydrocarbons and nitroaromatics) (Kappler and Haderlein, 2003) or heavy metals (e.g., Cr(VI) and Hg(II)) (Zhilin et al., 2004; Zhang et al., 2011; Graham et al., 2012). In addition, DOM may act as redox buffer through accepting electrons from microbial respiration under anoxic condition, and donating electrons to nitrate, iron, and sulfate, which may significantly contribute to the decrease of methanogenesis (Cervantes et al., 2000; Heitmann et al., 2007). To further understand the role DOM plays in the natural environment, we need to learn more about its electrochemical characteristics. It has been pointed out that EAC and EDC investigated through chronoamperometry can reflect the redox capacity of DOM, which results from a complex mixture of redox labile compounds and moieties with different redox characteristics (Nurmi and Tratnyek, 2011). Also, to explain what causes the differences in electron transfer capacity, we need to isolate the effects of specific redox-active functional groups, which justifies the use of voltammetry, another widely used electrochemical method. The results from DPV indicated at least 3 groups of redox-active moieties in DOM extracted from the forest soil, which can be quinones, phenols, organosulfur moieties and complexed metals as pointed out in previous studies (Ratasuk and Nanny, 2007; Nurmi and Tratnyek, 2011). Electrochemical reversibility which depends on the properties of the compound is typically represented by pairs of cathodic and anodic peaks in cyclic voltammograms (Nurmi and Tratnyek, 2002). In this study, unsymmetrical pairs of peaks with larger cathodic than anodic current in the cyclic voltammogram (**Fig. 3b**) testified that the redox moieties were partially reversible in electron transfer. Symmetrical peaks in cyclic voltammogram often are not observed because some redox couples are not fully reversible and/or side reactions may occur with the redox couple (Nurmi and Tratnyek, 2011).

Quinone moieties widely presenting in humus and humic-like substances are released into soils by plants and microorganisms (Scott et al., 1998; Ratasuk and Nanny, 2007) and have three redox states: oxidized (or benzoquinone), semiquinone radical, and reduced (or hydroquinone). Transformation between benzoquinone, semiquinone and hydroquinone is accompanied with electron transfer (Cory and Mcknight, 2005). Numerous studies employing excitation emission matrix (Cory and Mcknight, 2005), electron spin resonance (Scott et al., 1998), and cyclic voltammetry (Nurmi and Tratnyek, 2002) have provided multiple lines of evidence for the presence of redox active quinone moieties in DOM. In addition, it is thermodynamically favorable for most quinones to shuttle electrons from the bulk electron donors to the terminal acceptors (Tratnyek et al., 2001). The majority of present day investigators favor a humification mechanism that lignin during microbiological attack undergoes enzymatic conversion to quinones, which polymerize in the presence or absence of amino compounds to form humic-like macromolecules. In the upper layer, there is high microbial activity and enough organic materials for mineralization and then humification, which results in a high content of quinone moieties in DOM. Herein, DOM from an upper layer has a higher ETC (**Fig. 3**) and a higher HIX and fluorescence intensity. The results were yet another sign indicating that ETC of DOM was associated with humic-like substances which are rich in quinone moieties. Soil carbon pool dynamics not only is important for the productivity and sustainability of terrestrial ecosystems, but also contribute significantly to global carbon cycling (Chen et al., 2004). Growing concern about climate change has evoked interest in the role of DOM in the global carbon balance. In forest ecosystems, large internal DOM fluxes in soils relative to small outputs may result in carbon stabilization, thus, accumulation in the soil (Kaiser and Guggenberger, 2000). Therefore, numerous researchers have focused on the degradation and adsorption or/and co-precipitation of DOM which is a part of the carbon cycle (Kalbitz and Kaiser, 2008). As quinone-respiring is the dominate degradation pathway for DOM in the subsoil (Cervantes et al., 2000). ETC is an important parameter denoting the intensity of such anaerobic carbon respiration (Heitmann et al., 2007). As shown in **Fig. 2**, extremely small ETC of DOM in subsoil gave another evidence that DOM in the subsoil is less degradable (Kalbitz and Kaiser, 2008), which is beneficial to soil fertility preservation, soil carbon storage, and subsequently greenhouse gas reduction and global warming mitigation.

4 Conclusions

In this study, electrochemical approaches combined with spectroscopic methods were applied to evaluate the characteristics of DOM extracted along a forest soil profile. The

amounts and kinds of redox-active moieties in DOM and the electron transfer capacity of DOM decreased rapidly down the profile. These results gave evidence that soil acted towards DOM as a chromatographic system with DOM from an upper layer containing more humic-like substances rich in redox-active moieties. Electrochemical and spectral results give insight into the migration and transformation of DOM down a soil profile and aid to better understand the biogeochemical role of DOM in natural environments.

Acknowledgments

This work was supported by the National Natural Science Foundation of China (No. 41101211, 41071157, 41171205), and the Foundation for Excellent Young Scientist in Guangdong Academy of Sciences (No. rcjj201101).

References

Bauer I, Kappler A, 2009. Rates and extent of reduction of Fe(III) compounds and O_2 by humic substances. *Environmental Science and Technology*, 43(13): 4902–4908.

Bauer M, Heitmann T, Macalady D L, Blodau C, 2007. Electron transfer capacities and reaction kinetics of peat dissolved organic matter. *Environmental Science and Technology*, 41(1): 139–145.

Bi X Y, Ren L M, Gong M, He Y S, Wang L, Ma Z D, 2010. Transfer of cadmium and lead from soil to mangoes in an uncontaminated area, Hainan Island, China. *Geoderma*, 155(1-2): 115–120.

Blodau C, Bauer M, Regenspurg S, Macalady D, 2009. Electron accepting capacity of dissolved organic matter as determined by reaction with metallic zinc. *Chemical Geology*, 260(3-4): 186–195.

Cawley K M, Ding Y, Fourqurean J, Jaffé R, 2012. Characterising the sources and fate of dissolved organic matter in Shark Bay, Australia: a preliminary study using optical properties and stable carbon isotopes. *Marine and Freshwater Research*, 63(11): 1098–1107.

Cervantes F J, van der Velde S, Lettinga G, Field J A, 2000. Competition between methanogenesis and quinone respiration for ecologically important substrates in anaerobic consortia. *FEMS Microbiology Ecology*, 34(2): 161–171.

Chen C R, Xu Z H, Mathers N J, 2004. Soil carbon pools in adjacent natural and plantation forests of subtropical australia. *Soil Science Society of America Journal*, 68(1): 282–291.

Chen W, Westerhoff P, Leenheer J A, Booksh K, 2003. Fluorescence excitation-emission matrix regional integration to quantify spectra for dissolved organic matter. *Environmental Science and Technology*, 37(24): 5701–5710.

Chen X, Xia X H, Wu S, Wang F, Guo X J, 2010. Mercury in urban soils with various types of land use in Beijing, China. *Environmental Pollution*, 158(1): 48–54.

Chen Z, McGill W B, Dudas M J, Xing B, 1996. α-naphthol sorption as regulated by structure and composition of organic substances in soils and sediments. *Canadian Journal of Soil Science*, 76(4): 513–522.

Corvasce M, Zsolnay A, D'Orazio V, Lopez R, Miano T M, 2006. Characterization of water extractable organic matter in a deep soil profile. *Chemosphere*, 62(10): 1583–1590.

Cory R M, Mcknight D M, 2005. Fluorescence spectroscopy reveals ubiquitous presence of oxidized and reduced quinones in dissolved organic matter. *Environmental Science and Technology*, 39(21): 8142–8149.

Graham A M, Aiken G R, Gilmour C C, 2012. Dissolved organic matter enhances microbial mercury methylation under sulfidic conditions. *Environmental Science and Technology*, 46(5): 2715–2723.

Guo W D, Xu J, Wang J P, Wen Y R, Zhuo J F, Yan Y C, 2010. Characterization of dissolved organic matter in urban sewage using excitation emission matrix fluorescence spectroscopy and parallel factor analysis. *Journal of Environmental Sciences*, 22(11): 1728–1734.

Heitmann T, Goldhammer T, Beer J, Blodau C, 2007. Electron transfer of dissolved organic matter and its potential significance for anaerobic respiration in a northern bog. *Global Change Biology*, 13(8): 1771–1785.

Huo S L, Xi B D, Yu H C, He L S, Fan S L, Liu H L, 2008. Characteristics of dissolved organic matter (DOM) in leachate with different landfill ages. *Journal of Environmental Sciences*, 20(4): 492–498.

Kaiser K, Guggenberger G, 2000. The role of DOM sorption to mineral surfaces in the preservation of organic matter in soils. *Organic Geochemistry*, 31(7-8): 711–725.

Kaiser K, Kalbitz K, 2012. Cycling downwards-dissolved organic matter in soils. *Soil Biology and Biochemistry*, 52: 29–32.

Kalbitz K, Kaiser K, 2008. Contribution of dissolved organic matter to carbon storage in forest mineral soils. *Journal of Plant Nutrition and Soil Science*, 171(1): 52–60.

Kalbitz K, Schwesig D, Rethemeyer J, Matzner E, 2005. Stabilization of dissolved organic matter by sorption to the mineral soil. *Soil Biology and Biochemistry*, 37(7): 1319–1331.

Kanokkantapong V, Marhaba T F, Panyapinyophol B, Pavasant P, 2006. FTIR evaluation of functional groups involved in the formation of haloacetic acids during the chlorination of raw water. *Journal of Hazardous Materials*, 136(2): 188–196.

Kappler A, Haderlein S B, 2003. Natural organic matter as reductant for chlorinated aliphatic pollutants. *Environmental Science and Technology*, 37(12): 2714–2719.

Lovley D R, Coates J D, BluntHarris E L, Phillips E J P, Woodward J C, 1996. Humic substances as electron acceptors for microbial respiration. *Nature*, 382(6590): 445–448.

Nurmi J T, Tratnyek P G, 2002. Electrochemical properties of natural organic matter (NOM), fractions of NOM, and model biogeochemical electron shuttles. *Environmental Science and Technology*, 36(4): 617–624.

Nurmi J T, Tratnyek P G, 2011. Electrochemistry of natural organic matter. In: Aquatic Redox Chemistry (Tratnyek P G, Grundl T J, Haderlein S B, eds.). American Chemical Society, Washington DC. 129–151.

Ratasuk N, Nanny M A, 2007. Characterization and quantification of reversible redox sites in humic substances. *Environmental Science and Technology*, 41(22): 7844–7850.

Rumpel C, Eusterhues K, Kögel-Knabner I, 2004. Location and chemical composition of stabilized organic carbon in

topsoil and subsoil horizons of two acid forest soils. *Soil Biology and Biochemistry*, 36(1): 177–190.

Scott D T, McKnight D M, Blunt-Harris E L, Kolesar S E, Lovley D R, 1998. Quinone moieties act as electron acceptors in the reduction of humic substances by humics-reducing microorganisms. *Environmental Science and Technology*, 32(19): 2984–2989.

Tratnyek P G, Scherer M M, Deng B L, Hu S D, 2001. Effects of natural organic matter, anthropogenic surfactants, and model quinones on the reduction of contaminants by zero-valent iron. *Water Research*, 35(18): 4435–4443.

Yuan T, Yuan Y, Zhou S G, Li F B, Liu Z, Zhuang L, 2011. A rapid and simple electrochemical method for evaluating the electron transfer capacities of dissolved organic matter. *Journal of Soils and Sediments*, 11(3): 467–473.

Zhan X H, Wu W Z, Zhou L X, Liang J R, Jiang T H, 2010. Interactive effect of dissolved organic matter and phenanthrene on soil enzymatic activities. *Journal of Environmental Sciences*, 22(4): 607–614.

Zhang H C, Weber E J, 2009. Elucidating the role of electron shuttles in reductive transformations in anaerobic sediments. *Environmental Science and Technology*, 43(4): 1042–1048.

Zhang W, Li Q M, Wang X X, Ding Y, Sun J X, 2009. Reducing organic substances from anaerobic decomposition of hydrophytes. *Biogeochemistry*, 94(1): 1–11.

Zhang Y T, Chen X, Yang Y K, Wang D Y, Liu X, 2011. Effect of dissolved organic matter on mercury release from water body. *Journal of Environmental Sciences*, 23(6): 912–917.

Zhilin D M, Schmitt-Kopplin P, Perminova I V, 2004. Reduction of Cr(VI) by peat and coal humic substances. *Environmental Chemistry Letters*, 2(3): 141–145.

Zhou L X, Zhou S G, Zhan X H, 2004. Sorption and biodegradability of sludge bacterial extracellular polymers in soil and their influence on soil copper behavior. *Journal of Environment Quality*, 33(1): 154–162.

Zsolnay Á, 2003. Dissolved organic matter: artefacts, definitions, and functions. *Geoderma*, 113(3-4): 187–209.